Royal Norwegian Council
for Scientific and Industrial Research
(NTNF)

NORSAR

NORSAR Scientific Report No. 2-88/89

Semiannual Technical Summary

1 October 1988 – 31 March 1989

L.B. Loughran (ed.)

Kjeller, July 1989

VII.2 Continuous monitoring of seismic event detection capability

Introduction

In this paper we address the problem of using a network to continuously monitor the seismic noise field. The purpose is to determine to which extent interfering events affect the monitoring of events within a target region. We develop a model that can be used to obtain, at a given confidence level, a continuous assessment of the upper limit of magnitudes of seismic events in the target region that would go undetected by such a network. We give an example of application using data from the network of three regional arrays, NORESS, ARCESS, FINESA in Fennoscandia. The application of the model to more general problems in seismic monitoring is also briefly discussed.

Model

In formulating the approach, we consider a given geographical location, and a given "origin time" of a hypothetical event. Assume that this "target area" is to be monitored by a given seismic network, and that we wish to consider N seismic phases (there might be several phases per station).

For each phase, we assume that we have an estimate S_i of the signal (or noise) level at the predicted arrival time. For P-phases, S_i might be the maximum short term average (STA) value (1 second integration window) within $\pm$ 5 seconds of the predicted time. For Lg, a longer STA integration window (e.g., 10 seconds) might be used, and its maximum might be selected allowing a somewhat greater deviation from the predicted arrival time.

We assume that the network has been calibrated (or alternatively that standard attenuation values are available), so that magnitude correction factors (b_i) are available for all phases. Thus, if a detectable signal is present:

$$m_i = \log (S_i) + b_i \qquad (i = 1,2,...N) \qquad (1)$$

Here, m_i are estimates of the event magnitude m. Statistically, we can consider each m_i as sampled from a normal distribution (m,σ). Based on NORSAR experience, we consider a standard value of $\sigma = 0.2$ to be reasonable for a small epicentral area, and this value will be used in the following.

Let us now assume a "noise situation", i.e., that there are no phase detections corresponding to events at the given location for the given origin time.

We then have a set of "noise" observations a_i, where (see Fig. VII.2.1):

$$a_i = \log(S_i) + b_i \qquad (i = 1,2,...N) \qquad (2)$$

If a hypothetical event of magnitude m were present, it would have phase magnitudes m_i normally distributed around m. We know that for each phase,

$$m_i \leq a_i \qquad (i = 1,2,...N) \qquad (3)$$

Following a procedure similar to that of Ringdal (1976), we now consider the function:

$$f(m) = \text{Prob}(\text{all } m_i \leq a_i \ / \ \text{event magnitude m}) \qquad (4)$$

For each phase, we obtain probability functions $f_i(m)$ and $g_i(m)$ as follows:

$$f_i(m) = \text{Prob}(m_i \leq a_i/m) = 1 - \Phi \left(\frac{m-a_i}{\sigma} \right) \qquad (i=1,2,...,N) \qquad (5)$$

$$g_i(m) = \text{Prob}(m_i > a_i/m) = \Phi\left(\frac{m-a_i}{\sigma}\right) \quad (i=1,2,\ldots,N) \qquad (6)$$

where Φ is the standard (0,1) normal distribution.

Thus, assuming independence,

$$f(m) = \prod_{i=1}^{N} f_i(m) \qquad (7)$$

The probability g(m) that at least one of the observed noise values would be exceeded by the signals of a hypothetical event of magnitude m, then becomes

$$g(m) = 1 - f(m) \qquad (8)$$

As illustrated in Fig. VII.2.2, the 90 per cent upper limit is then defined as the solution of the equation

$$g(m) = 0.90 \qquad (9)$$

It is important to interpret the 90 per cent limit defined above in the proper way. Thus, it should not be considered as a 90 per cent network detection threshold since we have made no allowance for a signal-to-noise ratio which would be required in order to detect an event, given the noise levels. Rather, the computed level is tied to the actually observed noise values, and to the fact that any hypothetical signal must lie below these values. Our 90 per cent limit represents the largest magnitude of a possible hidden event, in the sense that above

this limit, there is at least a 90 per cent probability that one or more of the observed noise values would be exceeded by the signals of such an event.

Application to a regional network

As an application of the method, we selected as a target region to be monitored an area as shown in Fig. VII.2.3 situated at similar distance from the three arrays. For each of the three arrays, one Pn beam and one Lg beam were steered to this location. The beam traces were filtered using the frequency bands 3-5 Hz (Pn) and 2-4 Hz (Lg). Magnitude calibration values (b_i) were obtained by processing previously recorded events of known magnitude (M_L) and at similar distance ranges, and then determining b_i values independently for Pn and Lg.

Once these input traces had been formed from the three arrays, a set of time delays was introduced, using a delay for each phase that corresponded to the target location. Arrival time tolerances were set to $\pm$ 5 seconds for Pn and $\pm$ 10 seconds for Lg. This is roughly consistent with a beam radius of 50 km as shown on the figure. STA integration windows were set to 1 second for Pn and 10 seconds for Lg. The values of S_i in eq. (1) were obtained as the maximum STA values within the respective arrival time tolerances, using the mid-point of the integration interval as time reference.

We chose to analyze a 3 1/2 hour interval during which seven regional seismic events were reported in the Helsinki or Bergen bulletin. The highest magnitude (M_L = 2.9) corresponded to a large mining explosion at the USSR-Norway border close to the ARCESS site. These seven events were all located outside the target beam region, and one of our aims was to investigate how interfering signals from these events would influence the monitoring capability for the chosen beam region.

Fig. VII.2.4 shows, for the beam region considered, the computed 90 per cent upper magnitude limits, plotted as a function of time. In this

figure, only the Pn phase has been used, and the three arrays are shown individually and in combination (bottom trace).

It is clear from Fig. VII.2.4 that when considering individual arrays only, there are several possible time intervals when relatively large events (M_L ~ 2.0-3.0) located in the beam area might go undetected because of signals from interfering events. However, when the Pn phases are combined, these instances occur much more seldom.

Fig. VII.2.5 shows a similar plot, but this time including both the Pn and the Lg phase for each array. Even on an individual array basis, this causes substantial reduction in the upper magnitude limits. For the combined plot (bottom trace of Fig. VII.2.5), which takes into account all 6 Pn and Lg phases from the three arrays, we see that the upper limit is well below M_L = 2.0 for the entire time interval. Thus, we may conclude that, at the specified level of confidence, no event of M_L = 2.0 or higher occurred in the beam region during the time period considered.

Discussion

We consider that the method to provide continuous monitoring of upper magnitude limits at specified beam locations provides a useful supplement to standard statistical network capability studies (e.g., Wirth, 1977; Ringdal, 1986). In particular, this application would give a way to assess the possible magnitude of non-detected events during the coda of large earthquakes. In such situations, it would be appropriate to use global network data and include as many relevant phases as possible for each network station. For example, while an expected P phase at a given station may be obscured by the earthquake coda, later phases such as PcP or PP may be less influenced, and the noise level at their respective expected arrival times would therefore provide important information as to the size of possible undetected events.

We also note that the approach presented here to upper limit magnitude calculation could be applied to extend the utility of various discriminants, such as M_s:m_b. For small explosions, surface waves frequently are too weak to be observed at any station of the recording network. Obtaining reliable upper bound on M_s in such cases would expand the range of usefulness of this discriminant. In practice, an "upper bound" for single-station measurements has often been given as the "noise magnitude" at that station, i.e., the M_s value that corresponds to the actually observed noise level at the expected time of Rayleigh wave arrival. The proposed procedure will include this as a special case of a more general network formulation.

F. Ringdal
T. Kværna

References

Ringdal, F. (1976): Maximum-likelihood estimation of seismic magnitude. Bull. Seism. Soc. Am., 66, 789-802.

Ringdal, F. (1986): Study of magnitudes, seismicity and earthquake detectability using a global network. Bull. Seism. Soc. Am., 76, 1641-1659.

Wirth, M.H. (1977): Estimation of network detection and location capability. Teledyne Geotech, Alexandria, Virginia.

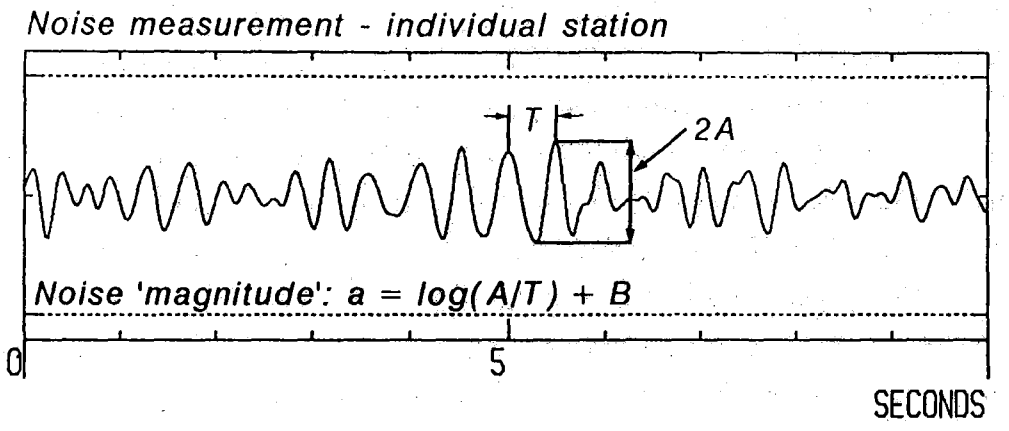

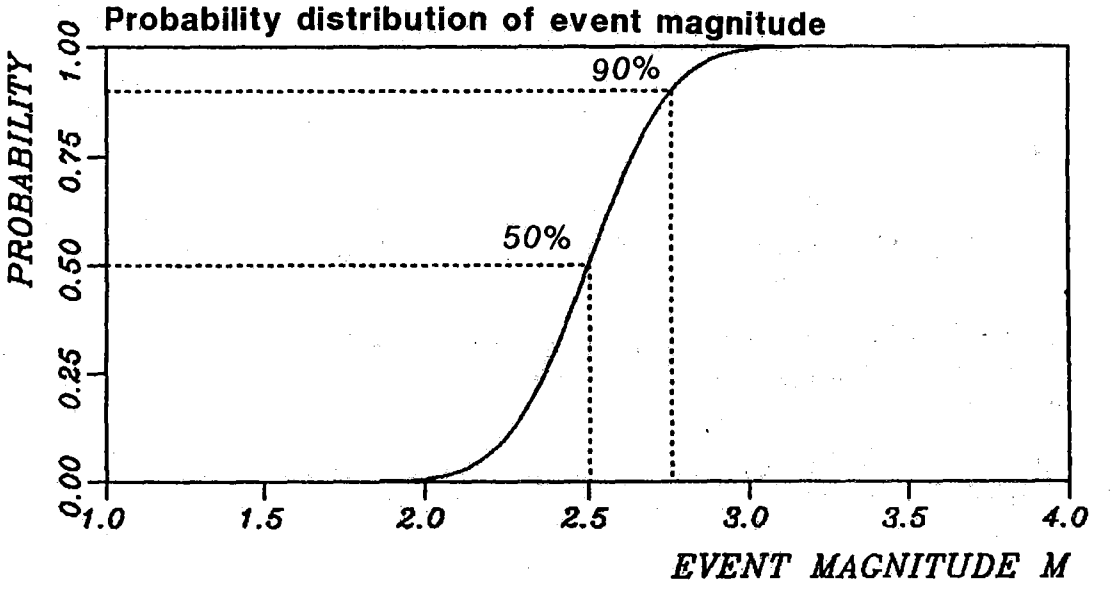

Fig. VII.2.1. Illustration of the method to calculate upper magnitude limits for the single station case. The top part of the figure shows how the noise "magnitude" is computed (given an assumed distance correction term B). The bottom part shows the corresponding probability function $g_i(m)$ defined in the text.

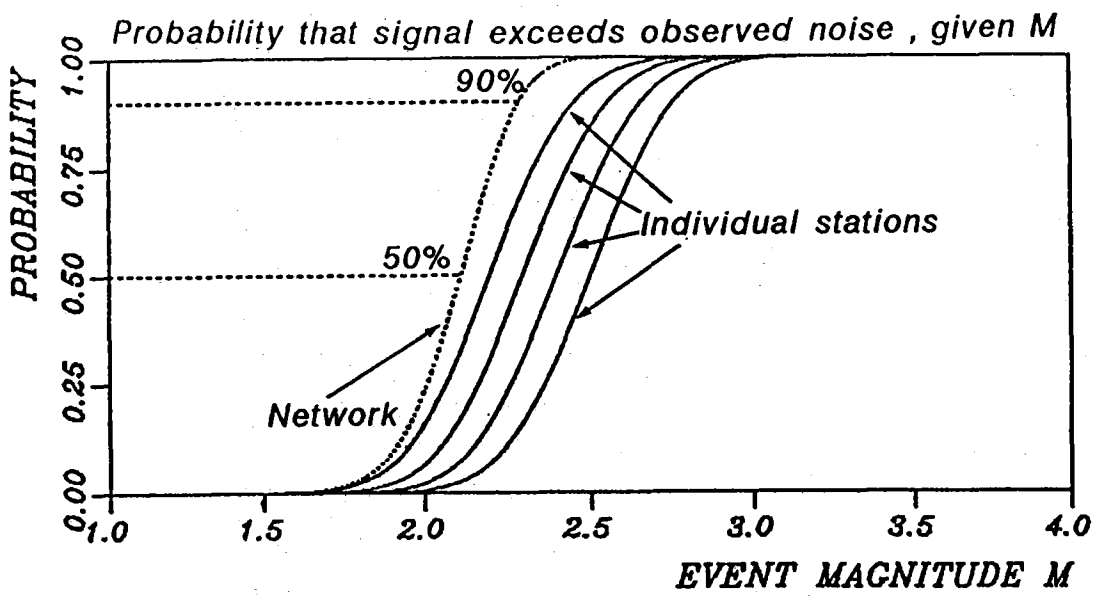

Fig. VII.2.2. Illustration of the procedure for calculating upper magnitude limits given a network of stations. Each network station gives rise to a probability distribution $g_i(M)$ as described in the text and illustrated in Fig. VII.2.1. The dotted curve, g(M), represents the probability, given event magnitude M, that the signal from a hypothetical event would exceed the actually observed noise level at at least one station.

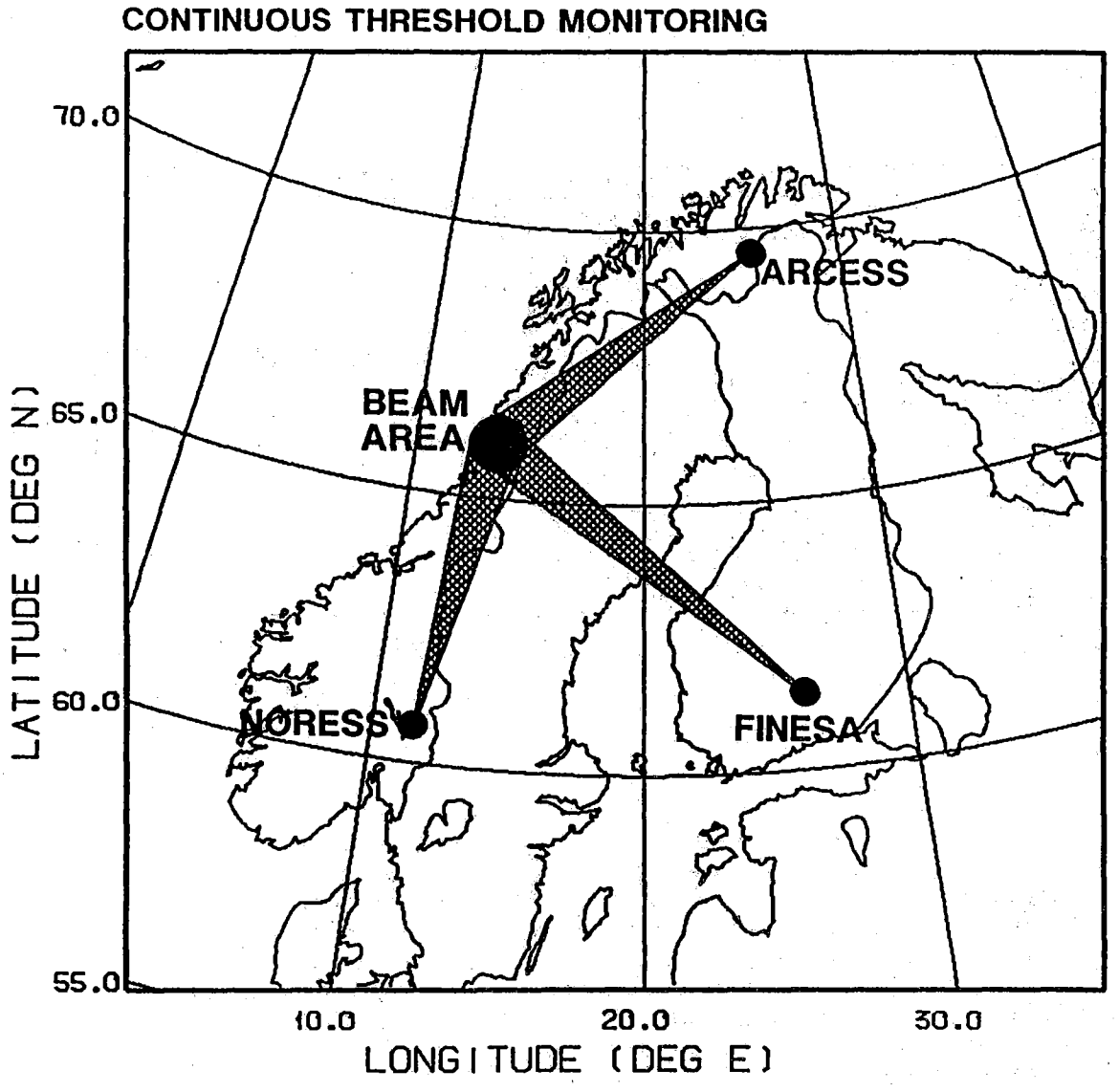

Fig. VII.2.3. Location of the beam area used in the example of continuous monitoring of upper magnitude limits on non-detected events. The area covers a circle of approximately 50 km radius, and is situated at similar distances from the three arrays.

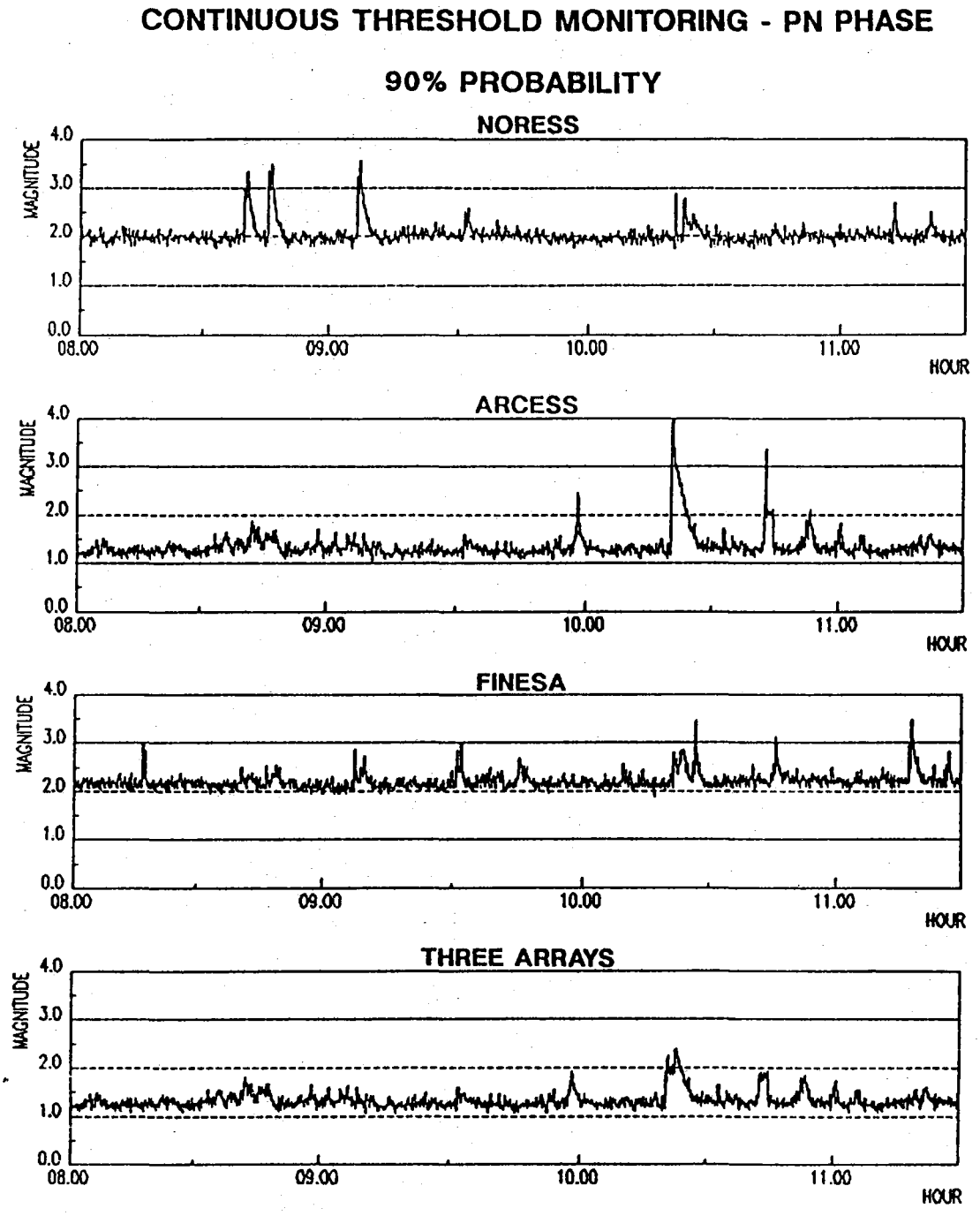

Fig. VII.2.4. Results from the continuous threshold monitoring of the area shown in Fig. VII.2.3 for a 3 1/2 hour period, using Pn phases only. The top three traces show, for each array, the largest magnitude of a possible non-detected event (confidence 90 per cent) as a function of time. The bottom trace shows the result of combining the observations from all three arrays (Pn phase only) as described in the text.

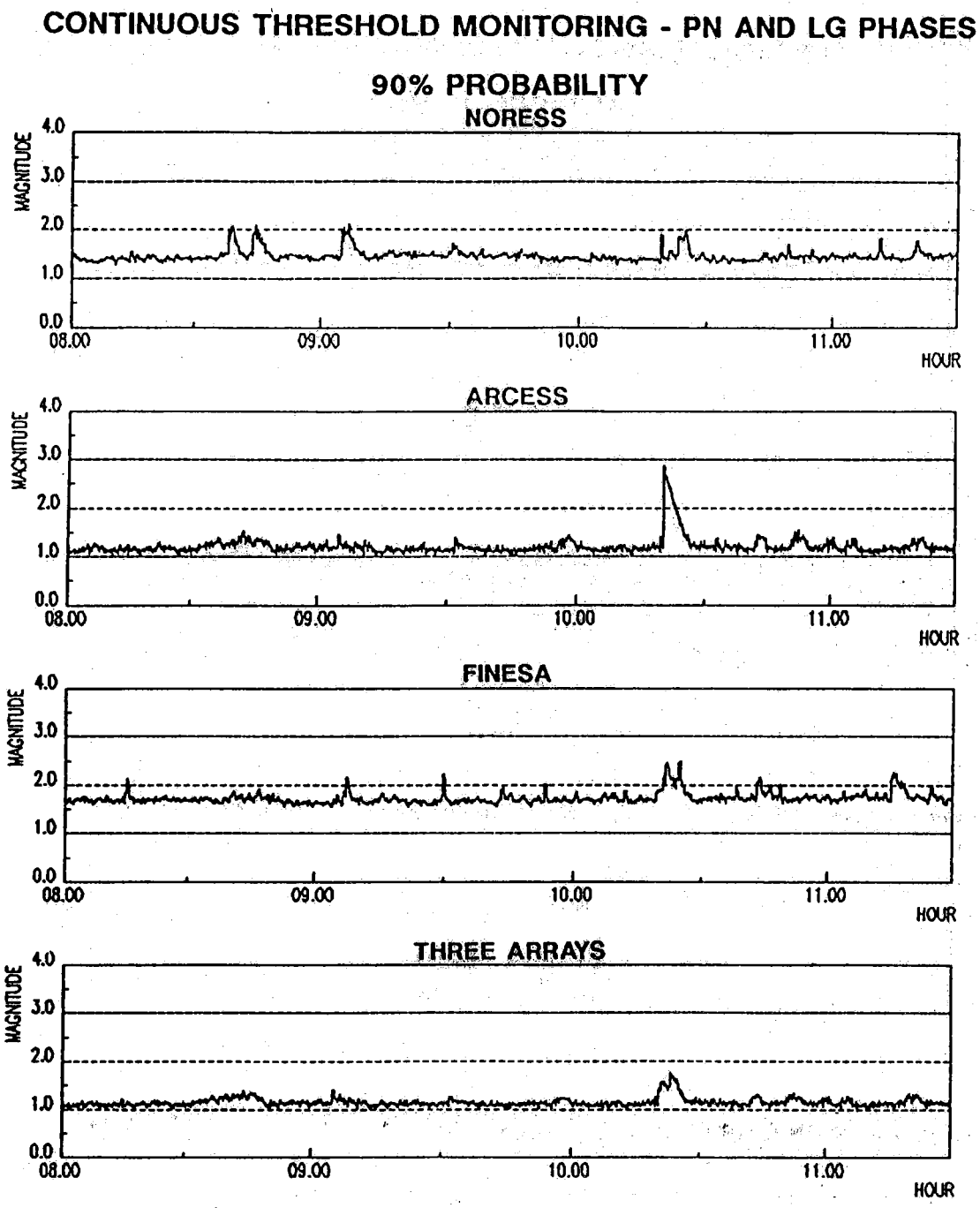

Fig. VII.2.5. Same as Fig. VII.2.4, but using both the Pn and Lg phases for the upper magnitude limit calculations. Comparing with Fig. VII.2.4, we note that this serves to lower the thresholds, both for each individual array (top three traces) and for the combined results (bottom trace).